Proceedings of the ASME 2013 Dynamic Systems and Control Conference
DSCC2013
October 21-23, 2013, Palo Alto, California, USA

DSCC2013-3782

ANKLE ANGLES DURING STEP TURN AND STRAIGHT WALK: IMPLICATIONS FOR THE DESIGN OF A STEERABLE ANKLE-FOOT PROSTHETIC ROBOT

Evandro M. Ficanha
emficanh@mtu.edu

Mohammad Rastgaar
rastgaar@mtu.edu

Barzin Moridian
bmoridia@mtu.edu

Nina Mahmoudian
ninam@mtu.edu

Department of Mechanical Engineering-Engineering Mechanics
Michigan Technological University, Houghton, Michigan 49931

ABSTRACT

*This article compares the three-dimensional angles of the ankle during step turn and straight walking. We used an infrared camera system (*Qualisys Oqus ®*) to track the trajectories and angles of the foot and leg at different stages of the gait. The range of motion (ROM) of the ankle during stance periods was estimated for both straight step and step turn. The duration of combined phases of heel strike and loading response, mid stance, and terminal stance and pre-swing were determined and used to measure the average angles at each combined phase. The ROM in Inversion/Eversion (IE) increased during turning while Medial/Lateral (ML) rotation decreased and Dorsiflexion/Plantarflexion (DP) changed the least. During the turning step, ankle displacement in DP started with similar angles to straight walk (-9.68° of dorsiflexion) and progressively showed less plantarflexion (1.37° at toe off). In IE, the ankle showed increased inversion leaning the body toward the inside of the turn (angles from 5.90° to 13.61°). ML rotation initiated with an increased medial rotation of 5.68° relative to the straight walk transitioning to 12.06° of increased lateral rotation at the toe off. A novel tendon driven transtibial ankle-foot prosthetic robot with active controls in DP and IE directions was fabricated. It is shown that the robot was capable of mimicking the recorded angles of the human ankle in both straight walk and step turn.*

INTRODUCTION

Straight walk requires a complex sequence of muscle activation to modulate the ground reaction forces to keep stability and produce forward motion. Similarly, modulation of the reaction forces to steer the body is required for turning [1]. Two different strategies are commonly used for turning. The spin turn consists of turning the body around the leading leg (e.g. turning right with the right leg in front). The step turn consists of shifting the weight to the leading leg and stepping in the opposite leg while still shifting the body (e.g. turning left with the right leg in front). The step turn is more stable since the base of support is wider [2] and for this reason it was used in this study. It has been shown that the step turn velocity, length, and width are considerably different than the straight walk with higher turning reaction forces [3]. Three-dimensional measurement of the ankle angles during step and spin turn have been previously studied [4]; however, it is of interest to study the ankle angles during heel strike, flat foot, and toe off during the step turn stages of the gait and also compare these results to the ankle angles during straight steps. Different approaches have been used to measure ankle angles such as using flexible electro-goniometer, electromagnetic tracking devices, and motion capturing cameras [2-6]. We used a motion capture camera system in this study.

Much research has focused on straight walk and the dorsi-plantarflexion of the ankle, while less attention has been given to the turning mechanism, although it plays a major role in locomotion [6]. As an example, amputees use their hip mainly in the sagittal plane to turn in such a way that the outside step length is longer than the inside step length, causing the body to rotate without the need to lean the body. Non-amputees rely mainly on ankle rotations in the sagittal plane and hip rotations in the coronal plane to tilt the body towards the inside of the turn [1]. It is estimated that the different strategies are required to compensate for the lack of propulsion in the passive prostheses to increase stability and maneuverability [1]. This evidence suggests that an ankle-foot prosthesis controllable in both dorsi-plantarflexion and inversion-eversion directions may provide more assistance in conforming the foot to the ground profile and uneven surfaces, walking in arbitrary directions on

the slopes, steering, and turning. Currently, there are few commercially available transtibial powered prostheses that actively control one degree of freedom (DOF) in the sagittal plane [7-9]. BiOM provides the necessary energy during toe-off (plantarflexion); therefore, it actively contributes in gait and lowers the metabolic cost. The controller in BiOM allows for gait in different cadences over surfaces with different inclination in uphill and downhill trajectories [7]. Proprio Foot from Ossur uses a stepper motor to provide dorsiflexion motion during swing forward and adjustment of the ankle angle on the surface with different trains. The controller uses a pattern recognition algorithm to adapt to the human's gait continuously [8]. Elan from Endolite uses a hydraulic ankle and the controller provides both dorsiflexion for foot clearance and plantarflexion for support during stance by adjusting the ankle joint resistance [9]. Humans, however, tend to regulate the joint movement for a low metabolism cost rather than its kinematic pattern [10]. The proposed design in this paper will advance the state-of-the-art ankle prostheses by providing a steering mechanism that enables control of two degrees of freedom of the ankle to potentially enhance the maneuverability and stability in amputees.

This paper describes the methodology used and the preliminary results of the three-dimensional rotations of the ankle during the stance period in straight walk and step turn. The motivation behind this study is to better understand the mechanism of turning and use it to develop a prosthetic ankle-foot robot with anthropomorphic characteristics and capable of steering and accommodating ground profile changes. Finally, we introduce the prototype of a prosthetic ankle-foot robot with a steering mechanism.

EXPERIMENT METHODOLOGY AND RESULTS

Human Subjects

Five male subjects with no self-reported neuromuscular and biomechanical disorders were recruited for the experiments (ages from 23 to 26 years and body mass index from 18.5 to 27.5). The subjects gave written consent to participate in the experiment that was approved by the Michigan Technological University Institutional Review Board.

Experimental Setup

A motion capture camera system was used to track the rotations of the foot and tibia. The system consisted of 8 cameras in a square formation with 4 cameras at the corners and 4 in between covering a volume of about 16 cubic meters and an area of 12 square meters. The cameras emitted infrared light and captured the reflected light from reflectors mounted on the participants with a rate of 250 Hz. Three reflectors are sufficient for the camera system to calculate the position and orientation of a rigid body if each reflector is visible to at least three cameras at that specific point at any time. To avoid the body obstructing the reflectors from being detected by enough cameras, each rigid body had a redundancy of reflectors. In the experiment, the subjects wore a shoe and a knee brace, each mounted with five reflective markers (Fig.1). The shoe and knee brace assured that the reflectors would not move with respect to each other as they would if they had been mounted on the skin or on the clothes of the participants.

The subjects were instructed to walk at a normal pace and an audible metronome was synchronized to their number of steps per minute in an attempt to keep the walking speed constant. The preferred speed for the participants ranged from 88 to 96 steps per minute.

FIGURE 1. KNEE BRACE AND SHOE WITH REFLECTORS. THE ARROWS POINT TO THE VISIBLE REFLECTORS.

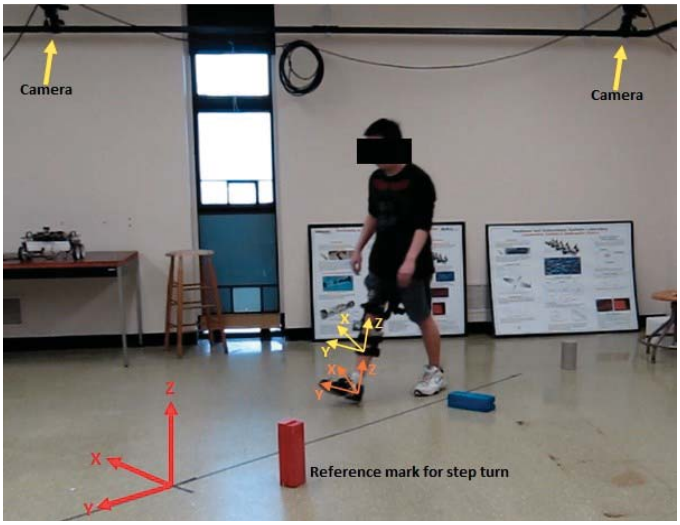

FIGURE 2. TEST AREA AND REFERENCE FRAMES. RED: GLOBAL REFERENCE FRAME OF THE WORK AREA. ORANGE: LOCAL REFERENCE FRAME OF THE FOOT. YELLOW: LOCAL REFERENCE FRAME OF THE LEG.

The subjects were instructed to walk from outside the field of view of the cameras while following a straight line marked on the floor. When they reached a reference point (Fig. 2) on the floor, they performed a 90° step turn to the left, pivoting on their right leg and continued walking straight until they were outside the field of view of the cameras. Several training trials were performed prior to the tests to ensure subjects were comfortable executing the step turn. In addition, subjects were asked to stand still in the center of the testing area, facing the

same walking direction as they entered the workspace. This way, the position of the reflectors in the foot and leg could be recorded to establish the local coordinate system of the rigid bodies, in addition to a right-handed global Cartesian coordinate system for the testing area. The global coordinate system is defined so the subject walks in the direction of the positive Y axis and turn left in the negative X axis direction (Fig. 2). The coordinate system needed to be established one time for each subject before they repeated the walking and turning test nine times. After recording the markers' trajectories, all the markers that were mounted on each object (i.e. shoe and knee brace) were defined as single objects and local coordinate systems were defined at the geometric center of each group of markers with the same orientations as the global reference frame. Another step was required to characterize the angles of the foot with respect to the leg. The result included position and orientation of the leg and foot relative to the global coordinate system in addition to position and orientation of the foot relative to the coordinate system of the leg.

To calculate the orientation of the foot and leg at each state of the gait, the rotation of the foot about the global X axis (Fig. 3) was used to estimate the heel strike (consisting of heel strike and loading response phases), flat foot (mid-stance phase), and toe-off (consisting of terminal stance and pre-swing phases) in each step. Note that the foot angle is positive before heel strike (the heel is on the ground and the toes are elevated), zero when the foot is flat on the ground, and negative at the toe-off (the heel is elevated and the toes are on the ground).

The global position of the foot in the Y axis was used to identify whether the step was a straight or a turning step, as well as to identify the start and the end of the stance periods. The increased displacement in the Y direction during the swing periods of the leg prior to the step turn was used as the indicator of the turn, as this displacement remained near constant after the step turn (Fig. 3).

The plots of DP, IE, and ML angles for a representative subject are shown in Fig. 4. The data for each test was divided into 6 segments (heel strike, flat foot, and toe-off from straight and turning steps) and the averages of the DP, IE, and ML angles of each segment were calculated for each of the 45 tests (9 tests on 5 subjects). Table 1 shows the average ROM for the straight step and step turn during the stance periods. Table 2 shows the average rotations and the difference in angles from the turning step to the straight step in each phase. The range of motion of each subject's ankle about the three axes of the ankle and their average rotations were calculated in each state of the walk. The subjects' range of motion was used to calculate the averaged percent change from straight walk to step turn with respect to their ROM in straight step (Table 2).

DISCUSSION

There was a modest decrease in DP ROM during the step turn compared to the straight step (Table 1). IE ROM increased

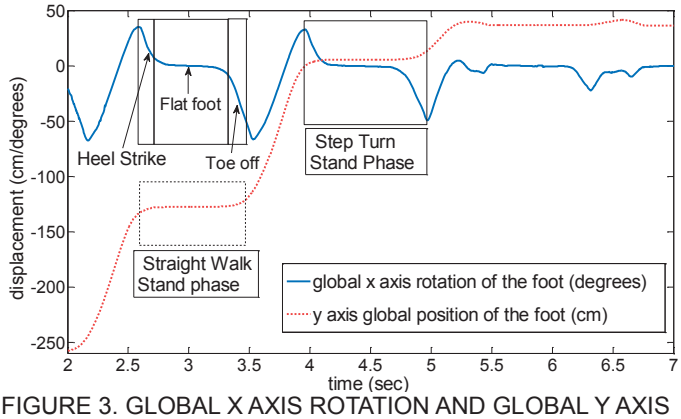

FIGURE 3. GLOBAL X AXIS ROTATION AND GLOBAL Y AXIS POSITION OF THE FOOT USED TO IDENTIFY DIFFERENT STATES OF THE GAIT.

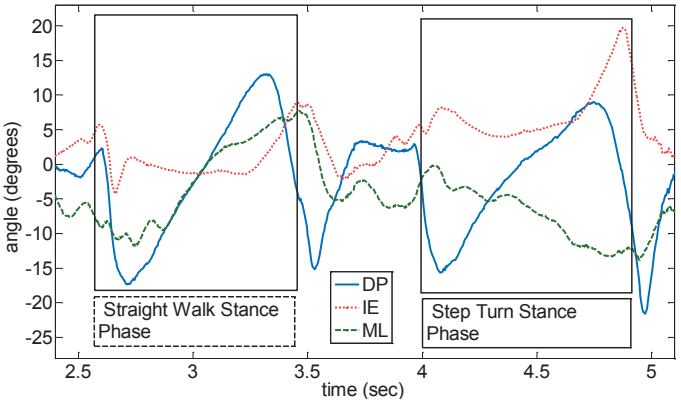

FIGURE 4. A REPRESENTATIVE SUBJECT'S ANKLE ROTATIONS IN DP, IE, AND ML DIRECTIONS DURING THE STRAIGHT STEP AND STEP TURN.

TABLE 1. RANGE OF MOTION OF ANKLE DURING THE STANCE IN STRAIGHT WALK AND STEP TURN

	ROM of Straight Step Stance Period (deg)		ROM of Step Turn Stance Period (deg)		% Change
	Degrees	Standard Error	Degrees	Standard Error	
DP	33.9	0.65	31.6	0.62	-7.4
IE	15.69	0.52	20.6	1.06	23.8
ML	22.09	0.6	16.8	0.65	-31.9

by 23.8% indicating an increase in IE role during steering. A significantly smaller range of motion in ML may suggest a higher stiffness in that axis of rotation necessary to transfer the reaction forces from the ground to the body.

As the step progressed through the gait, differences were observed between the straight step and step turn for all subjects. DP displacement started at a similar initial angle as the straight step (-9.68° of dorsiflexion) but progressively showed less plantarflexion (1.37° at toe-off compared to 10.37° in straight walk toe-off) indicating less forward propulsion. IE displacement started with 5.9° of inversion and increased to 13.6° at toe-off during the step turn suggesting a gradual increase in inversion to lean the body toward the inside of the

turn. At the heel strike of the step turn, ML displacement had an increase of 5.68° of medial rotation compared to straight walk, suggesting an anticipatory motion of the foot. The difference increased to 12.06° of lateral rotation at the toe-off generated by the pivoting of the body on top of the foot.

TABLE 2. AVERAGE ANGLES AT DIFFERENT PHASES OF STANCE IN STRAIGHT STEP AND STEP TURN

	Straight Step Average (deg)	Standard Error	Turning Step Average (deg)	Standard Error	Angular Change (deg)*	% Change**
DP heel Strike	-8.72	0.80	-9.68	0.95	-0.95	-3.0
DP flat foot	2.34	0.63	0.36	0.64	-1.98	-6.5
DP toe off	10.59	1.24	1.37	0.90	-9.22	-29.2
IE heel strike	-1.72	0.53	5.90	0.63	7.61	46.6
IE flat foot	-2.93	0.27	6.51	0.22	9.44	60.5
IE toe off	1.44	0.45	13.61	0.46	12.17	82.0
ML heel strike	-5.34	0.57	0.34	0.62	5.68	25.6
ML flat foot	-0.90	0.45	-3.55	0.41	-2.65	-12.8
ML toe off	5.53	0.32	-6.53	0.65	-12.06	-58.0

*Turning step angles – Straight step angles
**From straight to step turn with respect to individual straight walk ROM in stance period.

NOVEL CABLE-DRIVEN POWERED ANKLE-FOOT PROSTHESIS WITH TWO CONTROLLABLE DOF

The result from the ankle rotations in three DOF suggested that a steerable mechanism in prostheses may enhance the gait efficiency by allowing ankle inversion/eversion during step turn. A steerable transtibial prosthesis with powered ankle movement in two DOF was developed. The design feature is anticipated to enable the device to adapt to uneven and inclined grounds and participate in steering, allowing the amputees to benefit more from their prosthetic ankle-foot rather than using their hip joint to stabilize their gait and increase maneuverability in different terrains. Hence, a more natural gait may be feasible.

The prototype prosthesis (Fig. 5) consists of a socket that will be tailored to fit to the residual limb of the amputees (not shown), a pylon (A), two DC motors (E) and planetary gearheads (D) that are powered by two motor controllers (B) and receive signals from a DAQ board (M) connected to a remote computer and two quadrature encoders (I). Two cable drums (J) transfer the required torque to the ankle through the cable (K). A universal joint (F) connects the pylon to the foot and an elastic carbon-fiber plate. Both actuators apply the torque to the foot using a cable-driven mechanism with pulleys (C). The cable is attached to a carbon fiber plate (H) which is connected to the foot (L). In the rear side of the carbon fiber plate, the cable is mounted at both sides of the longitudinal axis of the foot. At the front side of the carbon fiber plate, the cable is passed through a pulley (G). The motors are powered by two motor controllers (B). The mechanism is capable of both dorsiflexion-plantarflexion when the motors rotate in opposite directions and inversion-eversion when the motors rotate in the same direction. Also, any combination of DP and IE can be obtainable by combining different amounts of rotation in each motor.

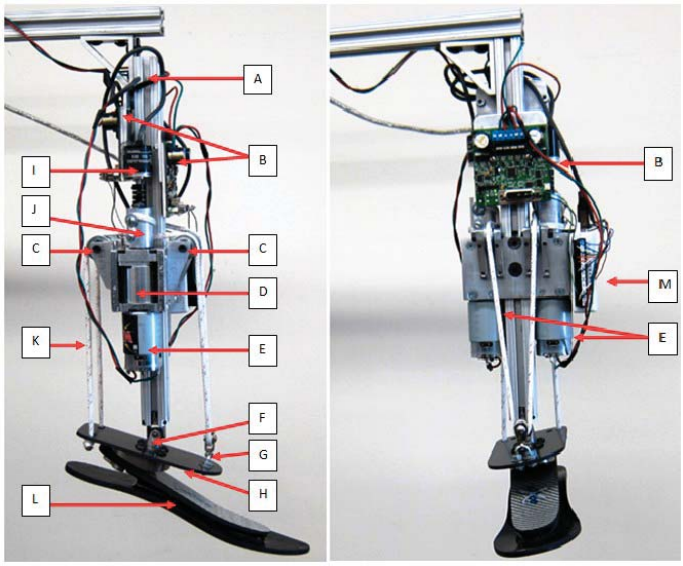

(A) (B)

FIGURE 5. PROTOTYPE OF A STEERABLE POWERED ANKLE-FOOT PROSTHESIS A- IN PLANTARFLEXION B-IN INVERSION

The energy consumption required at each step in an average able-bodied human weighing 70 kg is 36 J/step for walking (250 watts peak power) [11]. These amounts are 35% higher for an individual with a transtibial prosthesis [11, 12]; also, the prosthesis is estimated to have up to 40% losses resulting on an anticipated peak power consumption of 470 watts and an energy consumption of 68 J/step. Two brushed DC motors and motor controllers capable of a continuous torque output of 0.25Nm at 9200 RPM (producing 240 watts each for a total of 480 watts) were chosen to accommodate these requirements. Two 11.1 Volts LiPo batteries connected in series with an energy density of 572kJ/Kg are estimated to provide energy for 5800 steps. A planetary gear reduction with a 104:1 ratio was used to increase the delivery of the necessary torque in locomotion. The current prototype weighs 3 Kg without the battery and socket.

Presently, optical encoders provide position feedback to a remote computer that uses a proportional plus rate controller to mimic the angles captured with the motion camera system in both DP and IE. The input and output angles to the controller can be seen in Fig. 6 where the robot is moving at 50% of walking speed. For ease of comparison, the output plots have a time shift to remove the 80 milliseconds delay of the output. Also, all signals are filtered with a low-pass filter with a cutoff frequency of 5Hz to remove frequency components from the input that are beyond the bandwidth of the motors, and also to remove sensor noise from the output signal. The current prototype was developed as a proof-of-concept to validate the design kinematic; therefore, faster motors and sensors with lower noise levels will be used for the next design.

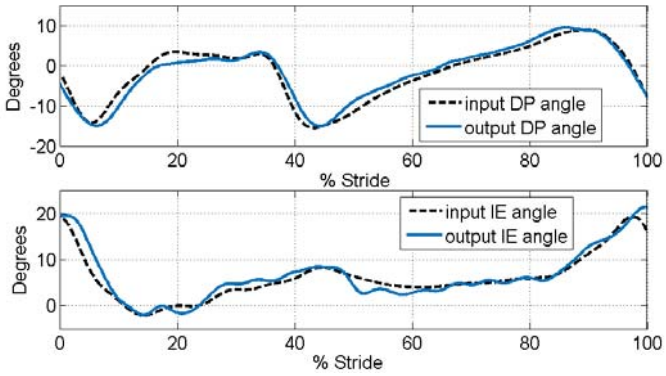

FIGURE 6. REGENERATED HUMAN ANKLE MOTION DURING A STEP TURN AND PRIOR SWING BY THE ANKLE-FOOT PROTOTYPE AT 50% OF WALKING SPEED AND NO LOAD.

FUTURE WORK

We will increase the number of subjects and also record the angles of the inside leg during straight walk and step turn. Additionally, the number of tests will be increased to assure the data is statistically significant.

Future robot designs will incorporate a selection of passive elements based on the characteristics of the ankle inertia, damping, and stiffness derived from the estimated impedance of the ankle [13-15]. This includes the replacement of the universal joint in the ankle by an elastomer providing anthropomorphic characteristics and passive stiffness in 3 DOF. The elastomer will provide stability that will allow the prosthesis to be used in case of battery exhaustion. The control of the ankle joint will be based on the control of the time-varying impedance of the ankle during different phases of stance period while providing the required torque. This approach is similar to the control approach suggested and implemented in [16]. In our prototype, however, the control algorithm will regulate the impedance in two DOF and the number of modes in the finite states control architecture will be determined based on the estimation of the time-varying ankle impedance at different phases of the stance period. A perturbation walkway is under development for collecting necessary data and the impulse response identification method will be used for estimation of the time-varying impedance of the ankle during gait [17]. Moreover, it is necessary to study the required features that allow transferring of the ankle generated moment in the frontal plane through the socket to the limb residue. Additionally, an optimal combination of sensors, including the force sensor under the socket, force sensors under the foot, and inertial measurement units, in conjunction with look-up tables of prerecorded data, will be utilized to identify the state of the gait, regulate the impedance, and deliver the necessary torque. A FPGA board will replace the remote computer of the current prototype and faster brushless motors with higher power-to-weight ratio and efficiency will be used to decrease the weight of the robot and its time delay, and increase battery life.

REFERENCES

[1] Ventura, J. D., Segal, A. D., Klute, G. K., and Neptune, R. R., 2011, "Compensatory Mechanisms of Transtibial Amputees During Circular Turning," Gait & Posture, 34, pp. 307–312.

[2] Hase, K., and Stein, R. B., 1999, "Turning Strategies During Human Walking," J Neurophysiol., 81(6), pp. 2914-2922.

[3] Glaister, B. C., Orendurff, M. S., Schoen, J. A., Bernatz, G. C., and Klute, G. K., 2008, "Ground Reaction Forces and Impulses During a Transient Turning Maneuver," J. Biomechanics, 41(4), pp. 3090-3.

[4] M.J.D. Taylor, P. D., S.C. Strike, 2005, "A Three-Dimensional Biomechanical Comparison between Turning Strategies During the Stance Phase of Walking," Human Movement Science, 24, pp. 558-573.

[5] Computing Community Consortium, March 20, 2013, A Roadmap for Us Robotics, from Internet to Robotics,

[6] Orendurff, M. S., Segal, A. D., Berge, J. S., Flick, K. C., Spanier, D., and Klute, G. K., 2006, "The Kinematics and Kinetics of Turning: Limb Asymmetries Associated with Walking a Circular Path," Gait & Posture, 23(1), pp. 106-111.

[7] 2012, Bionic Technology with Powered Plantar Flexion, www.iwalkpro.com/Prosthetists.html

[8] 2012, The Technology Behind the Proprio Foot® from Össur, www.ossur.com

[9] 2012, Endolite, Élan, www.endolite.com

[10] Kao, P. C., Lewis, C. L., and Ferris, D., 2010, "Invariant Ankle Moment Patterns When Walking with and without a Robotic Ankle Exoskeleton," Journal of Biomechanics, 43(2), pp. 203-209.

[11] Hitt, J. K., Sugar, T. G., Holgate, M., and Bellman, R., 2010, "An Active Foot-Ankle Prosthesis with Biomechanical Energy Regeneration," J. Med. Devices, 4(1).

[12] Rao, S. S., Boyd, L. A., Mulroy, S. J., Bontrager, E. L., Gronley, J. K., and Perry, J., 1998, "Segment Velocities in Normal and Transtibial Amputees: Prosthetic Design Implications.," IEEE Trans Rehabil Eng. , 6(2), pp. 219-26.

[13] Lee, H., Ho, P., Rastgaar, M., Krebs, H. I., and Hogan, N., 2011, "Multivariable Static Ankle Mechanical Impedance with Relaxed Muscles," Journal of Biomechanics, pp. 1901-1908.

[14] Rastgaar, M., Ho, P., Lee, H., Krebs, H. I., and Hogan, N., 2009, "Stochastic Estimation of Multi-Variable Human Ankle Mechanical Impedance," DSCC conference, Hollywood, CA.

[15] Rastgaar, M., Ho, P., Lee, H., Krebs, H. I., and Hogan, N., 2010, "Stochastic Estimation of the Multi-Variable Mechanical Impedance of the Human Ankle with Active Muscles," DSCC Conference, Boston, MA.

[16] Sup, F. C., 2009, "A Powered Self-Contained Knee and Ankle Prosthesis for near Normal Gait in Transfemoral Amputees," Ph.D. thesis, Vanderbilt University, Nashville, Tennessee.

[17] Lee, H., Krebs, H. I., and Hogan, N., 2012, "Linear Time-Varying Identification of Ankle Mechanical Impedance During Human Walking," DSCC Conference, Fort Lauderdale, FL.